Chemical Engineering Journal 517 (2025) 164196

Contents lists available at ScienceDirect

Chemical Engineering Journal

journal homepage: www.elsevier.com/locate/cej

# Robust strategy for bioplastic production from cyanobacteria-enriched microbiomes: insights from gene expression and population dynamics

Beatriz Altamira-Algarra [a], Lin Sun [a], David San León Granado [b,c], Lucía Romero-Morillo [a], Livia Vurro [a], Juan Nogales [b,c,d], Eva Gonzalez-Flo [a], Joan Garcia [e,*]

[a] GEMMA-Group of Environmental Engineering and Microbiology, Department of Civil and Environmental Engineering, Escola d'Enginyeria de Barcelona Est (EEBE), Universitat Politècnica de Catalunya-BarcelonaTech, Av. Eduard Maristany 16, Building C5.1, E-08019 Barcelona, Spain
[b] Department of Systems Biology, Centro Nacional de Biotecnología, CSIC, Madrid, Spain
[c] CNB DNA Biofoundry (CNBio), CSIC, Madrid, Spain
[d] Interdisciplinary Platform for Sustainable Plastics Towards a Circular Economy-Spanish National Research Council (SusPlast-CSIC), Madrid, Spain
[e] GEMMA-Group of Environmental Engineering and Microbiology, Department of Civil and Environmental Engineering, Universitat Politècnica de Catalunya-BarcelonaTech, c/ Jordi Girona 1-3, Building D1, E-08034 Barcelona. Spain

## 1. Introduction

Polyhydroxyalkanoates (PHA) represent a promising avenue as sustainable plastic alternatives due to its biodegradability and reduced environmental footprint [1]. Cyanobacteria stand out as an attractive platform for PHA synthesis, particularly in the form of Polyhydroxybutyrate (PHB), offering autotrophic production using sunlight and atmospheric $CO_2$ or industrial flue gases. Cyanobacteria accumulate PHB under nutrient-limited conditions, but generally achieving low content, up to date typically less than 10 % dry cell weight (dcw) [2–7]. In contrast, optimizing cultivation methods is crucial for boosting yields and facilitating process scale-up. Various studies have demonstrated potential in augmenting biopolymer synthesis through approaches such as supplementation with organic carbon sources or implementing light–dark cycles instead of continuous illumination [8–10]. These strategies have successfully increased PHB content to as high as 38 % dcw in the cyanobactera *Synechocystis* sp., achieved through a combination of phosphorus deficiency, gas exchange limitations, and the supplementation with fructose and acetate [11].

While cyanobacterial biotechnology has shown significant promise across diverse sectors such as bioenergy, biotechnology, and agriculture [12–14], a key challenge persists: achieving stable, long-term bioproduction cultures while minimizing contamination. Up to now, most experiments have been conducted in sterile laboratory setups and typically lasting only a few days or weeks [5,7,11,15]. Studies at larger scale indicate that scaling up cyanobacteria cultures in non-sterile environments is possible [16–20]. Despite this feasibility, PHB yield in these larger systems remained relatively low, with the highest reported yield being 13 %dcw PHB over 75 days [16]. A notable difference between large and lab-scale photobioreactors (PBRs) is the impossibility to sterilize the former. This limitation suggests that using cyanobacterial microbiomes—a diverse microbial culture comprising various cyanobacterial strains and other microorganisms—rather than axenic monocultures, could be a promising alternative. Microbiomes offer an increased resilience to environmental fluctuations and a reduced susceptibility to contamination. Exploring the potential of microbial consortia in PHA production is an active and expanding field. For instance, studies have investigated the use of heterotrophic bacteria found in municipal activated sludge or aerobic granular sludge [21,22] as well as mixed cultures enriched with phototrophic organisms like purple phototrophic bacteria and cyanobacteria [23,24].

In this context, previous work [25] demonstrated the potential of a photosynthetic microbiome enriched in cyanobacteria for continuous PHB production over 108 days using a two-phase cultivation strategy in a 2.5 L PBR. This approach decoupled cell growth (phase 1, biomass maximization) from biopolymer accumulation (phase 2, triggering and maximizing intracellular PHB accumulation in the pre-grown cells). A key factor in achieving high PHB content was acetate supplementation in the dark, leading to reduced dissolved oxygen levels during the accumulation phase. The intracellular accumulation of PHB within cyanobacteria cells was confirmed by transmission electron microscopy and Nile Blue A staining, alongside the observed expression of crucial genes involved in PHB and glycogen metabolism. Furthermore, the extracted polymer was identified as PHB through Raman spectroscopy, Fourier-transform infrared spectroscopy (FTIR), and proton Nuclear Magnetic Resonance.

The PHB monomer content was also analysed employing Raman spectroscopy, Fourier-transform infrared spectroscopy (FTIR), and

* Corresponding author.
*E-mail address:* joan.garcia@upc.edu (J. Garcia).

https://doi.org/10.1016/j.cej.2025.164196
Received 10 April 2025; Received in revised form 19 May 2025; Accepted 26 May 2025
Available online 29 May 2025

proton Nuclear Magnetic Resonance to validate the extracted polymer as PHB.

Although some insights have been gained from studying the relationship between glycogen and PHB metabolites in the newly adopted PHB accumulation method, which combines acetate supplementation under dark conditions, little is known about the microbial dynamics and community composition that drive sustained, high PHB production. While previous research has focused on the metabolic pathways and conditions that promote PHB accumulation, an analysis of the microbial communities' present in these systems is currently lacking. This knowledge gap underscores the need for further investigation into the microbial factors that influence PHB yields.

Building on the previously established two-phase approach, which has proven effective for long-term continuous PHB production in cyanobacteria-enriched microbiomes, this study extends its application to a comparative analysis across four distinct photosynthetic microbiomes. Specifically, we aim to comprehensively investigate not only PHB production and its metabolic pathways but also, and crucially, to track the dynamic shifts in microbial populations over an extended 168-day continuous cultivation period – a timeframe rarely explored in such systems.

To achieve this, we applied the two-phase approach to four distinct photosynthetic microbiomes enriched in cyanobacteria, originally collected from water samples [26]. Experiments were conducted in 2.5 L PBR under non-sterile conditions, enabling the identification of a resilient microbiome capable of sustained PHB synthesis over a prolonged 168 days.

Beyond the evaluation of PHB production, this research also examined the interplay between glycogen and PHB metabolism through quantitative real-time PCR (RT-qPCR), allowing to assess gene expression differences across microbiomes with varying PHB content. To further understand the microbial dynamics, the microbiomes were characterized through 16S rRNA amplicon sequencing, tracking population shifts throughout the experiment. Finally, confocal laser scanning microscopy (CLSM) provided a detailed view of PHB granules within cyanobacterial cells, offering valuable insights into their intracellular distribution.

## 2. Materials and methods

### 2.1. Microbiome inoculums

Four microbiomes originally collected in [26] served as the inoculum for 3 L glass cylindrical PBRs. These PBRs were closed polymethacrylate cylinders with an 11 cm diameter and a working volume of 2.5 L. The sample codes established in [26] are used in this study. Microbiomes named R1 and R2 were obtained from the Besòs river (Sant Adrià de Besòs, Spain, 41°25′20.2″N 2°13′38.2″E), an intermittent Mediterranean stream receiving significant volumes of urban treated wastewater discharged from sewage treatment plants in the metropolitan area of Barcelona. Microbiomes named CW1 and CW2 originated from the constructed wetland in Can Cabanyes (Granollers, Spain, 41°34′06.8″N 2°16′09.4″E), which receives treated water from the wastewater treatment plant in Granollers [27]. To select cyanobacteria microbiomes, these samples were cultivated in BG-11 medium, as described in [5], with reduced phosphorus concentration (0.2 mg·$L^{-1}$) to favour growth of cyanobacteria over competing phototrophic organisms. Details of these cultures can be found in [26]. These inoculums were predominantly dominated by cyanobacteria species *Synechocystis* sp. and *Synechoccocus* sp. Bright light microscopy (Eclipse E200, Nikon, Japan) images of each microbiome are shown in Fig. A.1.

### 2.2. Experimental strategy

The methodology described in [25,28] based in repetitions (or cycles) of alternating cell-growth and PHB-accumulation phases was applied for 168 days to all microbiomes. Initially, a conditioning period consisting of a single repetition with one growth and PHB-accumulation phases was conducted. The growth phase started with the inoculation to each PBR with a biomass quantity to achieve a concentration of 100 mg volatile suspended solids (VSS)·$L^{-1}$ inside the reactor. BG-11 was used as culture medium as described in [5] with modified concentrations inorganic carbon (IC, as bicarbonate), nitrogen (N, as nitrate) and phosphorus (P, as phosphate) (100 mgIC·$L^{-1}$, 50 mgN·$L^{-1}$ and 0.1 mgP·$L^{-1}$, respectively). When nitrogen was depleted (after 20 days in conditioning period), the accumulation phase began. 600 mg acetate·$L^{-1}$ were added at this point to stimulate PHB production and PBRs were enclosed with PVC tubes to avoid light penetration and avoid photosynthesis and subsequent dissolved oxygen in the PBR. It is worth noting that we used the term "accumulation" and "starvation" interchangeably to denote the period when cells generate PHB in response to nutrient scarcity.

After this conditioning cycle, a total of ten repetitions were carried out for each microbiome, with each cycle consisting of 7 days in biomass growth phase and 7 days in PHB-accumulation phase. At the end of each repetition, a volume ranging from 800 mL to 1,200 mL was discarded from the PBRs to purge the culture broth and achieve an initial biomass concentration of approximately 400 mgVSS·$L^{-1}$ after the addition of fresh BG-11 medium (the same volume discarded). The BG-11 was prepared to achieve in the culture concentrations of 25 mgN·$L^{-1}$ and 0.1 mgP·$L^{-1}$. A daily dose of a solution of $KH_2PO_4$ was added to maintain phosphorus concentration at approximately 0.1 mgP·$L^{-1}$. The BG-11 added did not contain inorganic carbon (as bicarbonate) to promote the selection of cyanobacteria capable of producing PHB. The only source of inorganic carbon was from $CO_2$ injections used to control pH during the growth phase. This approach was based on the premise that cyanobacteria rely on internal carbon reserves, like glycogen or PHB. As a result, cells capable of synthesizing PHB/glycogen became dominant in the culture, outcompeting those that could not, due to the lack of external carbon substrates in the medium. At the beginning of the accumulation phase, 600 mg·$L^{-1}$ of acetate were added with the goal of triggering the production of acetyl-CoA and improving the PHB yields.

The experimental setup was consistent with the previously described in [25]. Reactors were continuously agitated by a magnetic stirrer to ensure complete mixing, and culture temperature was kept between 25 and 30 °C. Illumination was provided by a 200 W LED floodlight (positioned 15 cm from the reactor surface) at an intensity of approximately 420 μmol·$m^{-2}$·$s^{-1}$ (30 klx) with a 15:9h light:dark cycle during the growth phase. During the growth phase, the pH was actively controlled within a range of 7.5 to 8.3 using a pH control system (HI 8711, HANNA instruments). This system activated an electrovalve to inject $CO_2$ into the reactors when the pH reached 8.3, subsequently adjusting it back to values around 7.5. pH data were recorded at 5-minute intervals using the PC400 datalogger software (Campbell Scientific). During the accumulation phase, the pH was measured but not actively controlled as photosynthetic activity was minimal or absent under the experimental conditions of this phase (dark conditions as described previously).

### 2.3. Analytical methods

#### 2.3.1. Biomass, Nutrients and acetate analysis

During growth phases, biomass concentration was evaluated as VSS according to method 2540-D described in Standard Methods [29]. To provide a rapid estimation of biomass concentration during the accumulation periods, VSS was correlated with turbidity by calibration curve (Fig. A.2). Turbidity measurements were conducted employing a turbidimeter (HI93703, HANNA Instruments, Italy). VSS and turbidity measurements were done in triplicate.

Nitrogen analysis was conducted during the growth phase, following method 4500-$NO_3^-$ (B) from Standard Methods [29]. Note that in BG-11, the only source of nitrogen is nitrate. Prior to analysis, samples were filtered through a 0.7 μm pore glass microfiber filter to remove

particulates.

At the beginning and at the end of the accumulation phase, the concentration of acetate within the PBRs was determined too. Following the 0.7 μm filtration, samples were further filtered through a 0.45 μm PTFE filter. Acetate analysis was conducted using ion chromatography, with Metrohm's Eco IC instrument equipped with a Metrosep A Supp 19–250 4.0 column for anions. For the analysis, an eluent solution was employed containing 8 $mmol \cdot L^{-1}$ of sodium carbonate and 0.25 $mmol \cdot L^{-1}$ of sodium bicarbonate. The anion suppression solution used consisted of 250 $mmol \cdot L^{-1}$ sulfuric acid ($H_2SO_4$), 100 $mmol \cdot L^{-1}$ oxalic acid, and 5 % acetone (v/v).

### 2.3.2. PHB quantification

PHB analysis was performed at the initial and end point of each repetition. PHB was analysed using gas chromatography (GC) as described in [30]. Briefly, 50 mL samples were taken and centrifuged (3,000 g for 10 min). The cell pellet was first frozen at −80 °C overnight and subsequently freeze-dried for 24 h (−110 °C, 0.05 hPa) (ScanVac CoolSafe, LaboGene, Denmark). Freeze-dried biomass (3–3.5 mg) was mixed with 1 mL methanol solution containing $H_2SO_4$ (20 % v/v) and 1 mL chloroform ($CHCl_3$) containing 0.05 % w/w benzoic acid. The samples underwent heating for 5 h at 100 °C in a dry-heat thermo-block, followed by cooling in a cold-water bath for 30 min. Afterwards, 1 mL of deionized water was added, and the tubes were vortexed for 1 min. The $CHCl_3$ phase was recovered, and introduced into a GC vial with molecular sieves to remove traces of water. Analysis was conducted using a GC instrument (7820A, Agilent Technologies, USA) equipped with a DB-WAX 125–7062 column. Helium served as the gas carrier at a flow rate of 4.5 $mL \cdot min^{-1}$, with an injector split ratio of 5:1 and a temperature of 230 °C. The flame ionization detector temperature was set at 300 °C. Quantification of PHB was achieved using a standard curve derived from a co-polymer PHB-HV. The presence and quantity of co-copolymers were not investigated in this study.

### 2.3.3. Glycogen quantification

Samples for glycogen analysis were taken at the beginning and end of each repetition. Glycogen analysis was done by glycogen hydrolysis and measurements of the glucose produced following the method described by [31] with minor adjustments. In brief, freeze-dried biomass (2 mg) was mixed with 2 mL of 0.9 M HCl and digested for 3 h at 100 °C. Following digestion, the sample was centrifuged (12,000 g for 2 min) and the supernatant was filtered through a 0.45 μm pore size filter. Finally, glucose was analysed by anion exchange chromatography, using a Metrosep Carb 2–250/4.0 column (Agilent Technologies, USA), equipped with a pulsed amperometric detector. The eluent used was 300 mM sodium hydroxide and 1 mM sodium acetate. The analysis was conducted at 30 °C, at a flow rate of 0.5 mL $min^{-1}$. Glucose standards ranging from 5 to 100 ppm were used for calibration.

### 2.3.4. Microbial composition identification

Molecular characterization was performed to identify the species by clone library based on 16S rRNA gene amplification. Samples were taken at the following time points: the inoculum (referenced as day 0), start of the experiment (day 1), beginning of the accumulation of the conditioning cycle (day 20), and during repetitions two, four, six, eight, and ten (days 48, 76, 104, 132, and 160, respectively).

*2.3.4.1. DNA extraction.* DNA extraction was carried out using a modified protocol from [32] and applying the QIAsymphony Power-Fecal Pro DNA Kit (Qiagen, Germany). The DNA quality control was performed using Nanodrop equipment (ThermoFisher, Madrid, Spain) to ensure the DNA had the minimum conditions for extraction. DNA yield was calculated by measuring absorbance ratios spectrophotometrically, including A260/230 nm for salt and phenol contamination and A260/280 nm for protein contamination.

*2.3.4.2. 16S amplicon sequencing.* A total of 50 ng of DNA were amplified following the 16S Metagenomic Sequencing Library Illumina 15,044,223B protocol (ILLUMINA). V3 and V4 hypervariable regions of the bacterial 16S rRNA gene were amplified [33] and marked with a molecular identifier and performing a primer dimer cleanup. 16S based libraries were quantified by fluorimetry using Quant-iT™ PicoGreen™ dsDNA Assay Kit (Thermofisher). The libraries were sequenced on Illumina's Miseq platform combined with 300PE (Illumina, Madrid, Spain). A negative control containing water was obtained to confirm the absence of contamination. Illumina bcl2fastq2 Conversion Software v2.20 was used to demultiplex raw sequences.

*2.3.4.3. Sequencing data analysis.* Before sequence filtering and trimming, sequences were screened for contaminations, such as chloroplasts, using KRAKEN2 [34] the SILVA183 database, without any additional filtering. Next, sequences were filtered based on quality, and Illumina primers were trimmed. Only sequences with identified primers were retained for downstream analysis, allowing for amplicon reconstruction. PCR chimeras were removed using QIIME2-DADA2. Taxonomic annotation and abundance analysis were then performed using nf-core/ampliseq v2.10.0 [35] with Nextflow v20.05.0 and Docker, with the SILVA v183.1 database.

Downstream analysis was carried out using the Microeco R package [36]. The abundances from the ampliseq output were used to calculate relative abundances at the genus level using the Microeco trans_abund function, with results aggregated by color scale to the class level. To facilitate visualization, samples were grouped by microbiome and time point. The calculated abundances were then used as input of LegATO R package (https://github.com/wejlab/LegATo) to generate an alluvial plot.

To calculate the differential genus abundances, the trans_diff function from Microeco was used with the ANOVA method and a threshold of 0.001.

### 2.4. Confocal laser scanning microscopy

First, 2 mL culture samples were centrifuged (6,000 g for 4 min). Cell pellets were then rinsed three times with phosphate-buffered saline (PBS, 200 μL) and fixed with a solution (400 μL) of glutaraldehyde (2.5 % in PBS) for 15 min, followed by three additional washes in PBS. Finally, 1 % (wt/vol) Nile Blue A solution was used for PHB staining. Stained samples were observed with a 63X/1.4 numerical aperture oil immersion objective lens, excited with a diode 561 nm, and were viewed in a Carl Zeiss LSM 800.

### 2.5. RNA extraction and RT-qPCR

RT-qPCR analysis was conducted to assess the expression of genes involved in PHB and glycogen metabolism, as well as the tricarboxylic acid (TCA) cycle, reflecting the interconnected nature of these metabolic pathways. Specifically, the genes analysed were *phaC*, which codes for PHA synthase; *glgA*, responsible for glycogen synthase; *glgP1* and *glgP2*, encoding for glycogen phosphorylase; and *gltA*, encoding for citrate synthase. Primers were designed in a previous work using Primer-BLAST to specifically target the abovementioned genes in *Synechocystis* [37]. Given the significant differences in PHB production among microbiomes R1, R2, and CW2 compared to culture CW1, samples were collected only from CW2, representing lower PHB-producing cultures, and CW1, which exhibited elevated PHB synthesis.

Samples from microbiomes CW1 and CW2 were obtained at two distinct time points: (i) the start of the experiment (day 0), and (ii) on the last day of the accumulation phase of repetition 3 (corresponding to day 69 of the overall experimental timeline). Procedure described in [25] was followed with some modifications. Briefly, fresh biomass (50 mL) was harvested by centrifugation (14,000 rpm for 5 min at 4 °C) and

stored at – 80 °C in an ultra-freezer (ScanVac CoolSafe, LaboGene, Denmark). After thawing, were treated with lysozyme, homogenized in lysis buffer, incubated 5 min, and subjected to bead beating for lysis. RNA was isolated using the PureLink RNA Mini Kit (Ambion, ThermoFisher Scientific, USA) and quantified using a microplate reader (BioTek Synergy HTX, Agilent Technologies, USA). Genomic DNA was removed with DNaseI (ThermoFisher Scientific, USA). Reverse transcription was performed using the Revert Aid™ Kit (Thermo Fisher Scientific). The resulting complementary DNA was assessed for quality and quantity using a microplate reader (BioTek Synergy HTX, Agilent Technologies, USA).

Quantification of gene expression levels was achieved using the qPCR thermocycler QuantStudio 3 (ThermoFisher Scientific, USA), using the designed primers and concentration described in [37]. The *petA* gene was chosen as the housekeeping gene [37]. Each sample was analysed in triplicate for every gene.

For data analysis, the method by [38] was used. The mean Ct (mean cycle threshold, ΔCt) value represented the average difference between the Ct (cycle threshold) of the housekeeping gene and the gene of interest. The ΔΔCt value denoted the variation between the ΔCt value of each target gene and the mean ΔCt value of *petA* (housekeeping gene, reference). The mean ΔΔCt values for day 0 (inoculum, beginning of the experiment, control), and day 69 (day 7 of the accumulation phase, repetition 3) were calculated. Finally, the relative fold change in gene expression was calculated by:

$$\text{Fold gene expression} = 2^{-(\text{mean}\Delta\Delta\text{Ct})} \quad (1)$$

### 2.6. Statistical analysis

To evaluate differences in PHB content among microbiomes, data were analyzed using one-way analysis of variance (ANOVA), setting the significance level at $p < 0.05$. Prior to the ANOVA, a test for homogeneity of variances was conducted to ensure the validity of the assumptions underlying the ANOVA. Additionally, Tukey's method for multiple comparisons was applied in ANOVA's results to compare the mean values at the 95 % confidence level. Statistical analysis was performed using Minitab Statistical Software version 18.1.0.

To study the possible interaction between genes and the possible differences in gene expression analysis among microbiomes CW1 and CW2, statistical analysis was performed by Student's *t*-test followed by F- test. P-values $p < 0.05$ were considered statistically significant.

### 2.7. Calculations

Global kinetic coefficients for different microbiomes were calculated as follows:

Specific growth rate ($d^{-1}$) was calculated using the general formula:

$$\mu_X = \frac{\ln\left(\frac{X_{ti}}{X_{t0}}\right)}{t_i - t_0} \quad (2)$$

where $X_{ti}$ and $X_{t0}$ are the biomass concentration ($mgVSS{\cdot}L^{-1}$) at experimental day ($t_i$) and at the beginning of the growth phase ($t_0$), respectively. It is important to note that for $X_{ti}$, the values correspond to the day $t_i$ when the biomass concentration reached the stationary phase during growth, usually corresponding to the last day.

Biomass volumetric production rate ($mgVSS{\cdot}L^{-1}{\cdot}d^{-1}$) during growth phase was calculated as:

$$\Upsilon_{biomass} = \frac{X_{ti} - X_{t0}}{t_i - t_0} \quad (3)$$

Nitrogen (N) to biomass (X) yield was calculated only during the growth phase by:

$$Y_{X/N} = \frac{X_{ti} - X_{t0}}{N_{ti} - N_{t0}} \quad (4)$$

where $X_{ti}$ and $X_{t0}$ are the values at the end ($t_i$) and at the start of the growth phase ($t_0$). $N_{ti}$ ($mg{\cdot}L^{-1}$) and $N_{t0}$ ($mg{\cdot}L^{-1}$) represent the N concentration ($N\text{-}NO_3^-$) at the end ($t_i$) and at the start of the growth phase ($t_0$).

The specific consumption rate of nitrogen ($mgN{\cdot}gVSS^{-1}{\cdot}d^{-1}$) in the growth phase was determined as:

$$q_N = \frac{\mu_X}{Y_{X/N}} \quad (5)$$

PHB volumetric production rate (ϒPHB ($mgPHB{\cdot}L^{-1}{\cdot}d^{-1}$)) in the accumulation phase was obtained by:

$$\Upsilon_{PHB} = \frac{PHB_{tf} - PHB_{t0}}{t_f - t'_0} \quad (6)$$

where $PHB_{tf}$ and $PHB_{t0}$ are the concentration of PHB (in $mgPHB{\cdot}L^{-1}$) by the end ($t_f$) and at the beginning ($t'_0$) of the accumulation phase, respectively. These values were obtained multiplying the PHB yield on biomass ($\%_{dcw}PHB_{tf}$ and $\%_{dcw}PHB_{t0}$ in mg PHB·mg $VSSL^{-1}$) by the corresponding biomass concentration (in $mgVSS{\cdot}L^{-1}$).

The values for all these parameters are calculated as averages of the data obtained in each cycle.

## 3. Results and discussion

We investigated the potential of four cyanobacteria-rich microbiomes to produce PHB through a two-phase process, starting with biomass growth and followed by biopolymer accumulation, based on previous research [25,28]. Following an initial conditioning cycle, we conducted ten rounds, each lasting fourteen days—seven days for biomass growth and seven days for PHB accumulation. Using diverse analytical techniques (microscopy, gene expression analysis and 16S rRNA amplicon sequencing), we aimed to discern differences in gene expression and microbiome composition that contributed to varying PHB yields. Our goal was to differentiate the microbiomes and identify those most proficient in PHB production, capable of sustaining stable biopolymer synthesis over time.

### 3.1. Biomass evolution

The first cycle called "conditioning cycle" was done to set-up the experiment. Initially 50 $mgN\text{-}NO_3{\cdot}L^{-1}$ were added to each PBR to increase biomass concentration. During the growth phase of the conditioning, which lasted 20 days, nitrogen was progressively consumed to concentrations below 7 $mgN\text{-}NO_3{\cdot}L^{-1}$, leading to biomass concentration ranging between 800 and 1,300 $mgVSS{\cdot}L^{-1}$ depending on the microbiome (Fig. 1). To streamline PBRs operation, the growth phases of the subsequent ten cycles were reduced to 7 days each. For this purpose, and to ensure nitrogen exhaustion within this timeframe, a lower initial nitrogen concentration of 25 $mgN{\cdot}L^{-1}$ was used for each growth phase. This adjustment was based on successful results from previous work [25,28]. Upon the end of each growth phase, the biomass concentration across all reactors was around 520 and 620 $mgVSS{\cdot}L^{-1}$ (Fig. 1 and Table 1). Notably, the four microbiomes exhibited similar average specific growth rates (μ) throughout the different repetition cycles (Table 1). Among these, microbiome R1 showed the highest value with an average growth rate of $\mu$=0.06 $d^{-1}$. However, these growth rates are substantially lower than those reported in other mixed cultures enriched with cyanobacteria, where values have reached up to five times higher [25,39,40]. This discrepancy is likely linked to the specific cultivation conditions employed in this study. The sole reliance on $CO_2$ for pH adjustment combined with the significantly low phosphorus concentration (0.1 $mgP{\cdot}L^{-1}$), could have limited growth. Indeed, biomass

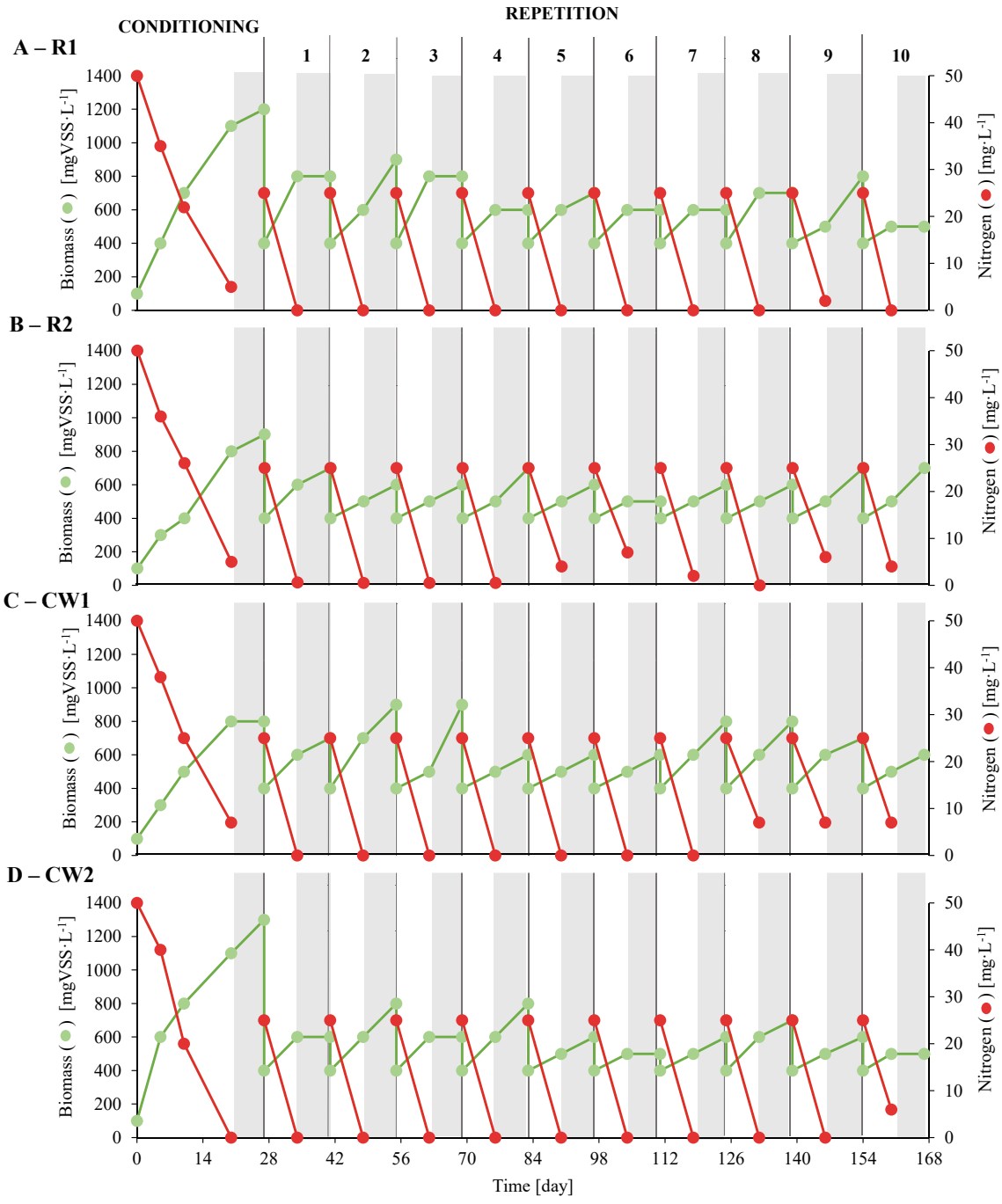


**Fig. 1.** Evolution of biomass (expressed as VSS) and nitrogen (as $NO_3$-N) concentrations for microbiomes (A) R1; (B) R2; (C) CW1; and (D) CW2. The white areas correspond to the growth phase. The onset of the accumulation phase in each cycle is marked by dashed vertical lines, with the grey area highlighting the duration of this phase. The completion of the cycle is indicated by solid vertical black lines.

growth and production are influenced by a range of factors, including strain variations, reactor configuration, culture medium, and environmental parameters such as nutrient levels, light intensity, and temperature [37,41,42]. For instance, a monoculture of the cyanobacteria *Synechocystis* sp. cultivated in nutrient-rich BG-11 medium (50 mgN·$L^{-1}$ and 5 mgP·$L^{-1}$) with bicarbonate as an inorganic carbon source achieved a growth rate of $\mu = 0.22\ d^{-1}$ and a biomass production rate of up to 150 mgVSS·$L^{-1}$·$d^{-1}$ [8]. This stark contrast highlights the potential influence of cultivation conditions.

### 3.2. PHB evolution

The evolution of PHB synthesis revealed distinct patterns across cultures and throughout the different cycles (Fig. 2 and Fig. A.3). Initially, all microbiomes displayed a limited PHB content. By the end of the accumulation phase of the conditioning cycle, microbiome R1 was the highest PHB producer, reaching a maximum of 9 %dcw PHB (108 mg·$L^{-1}$). During the ten-cycle experiment, differences in PHB synthesis abilities were observed among the four cultures. Remarkably, three microbiomes (R1, R2, and CW2) maintained consistent PHB synthesis, achieving an average biopolymer content ranging from 11 to 15 %dcw

**Table 1**
Averages and standard deviations of the global kinetic and stoichiometric parameters obtained by the end of the growth and the accumulation phase from the ten repetitions.

| | Microbiome | | | |
|---|---|---|---|---|
| | R1 | R2 | CW1 | CW2 |
| **Growth phase** | | | | |
| VSS [mg·L$^{-1}$] | 620 ± 23 | 520 ± 40 | 540 ± 88 | 550 ± 53 |
| μ [d$^{-1}$] | 0.06 ± 0.03 | 0.03 ± 0.01 | 0.04 ± 0.02 | 0.05 ± 0.01 |
| $\Upsilon_{biomass}$ [mgVSS·L$^{-1}$·d$^{-1}$] | 31 ± 18 | 17 ± 8.0 | 20 ± 12 | 22 ± 7.9 |
| $q_N$ [mgN·gVSS$^{-1}$·d$^{-1}$] | 7.2 ± 0.7 | 8.0 ± 0.5 | 7.5 ± 0.7 | 7.6 ± 0.4 |
| $Y_{X/N}$ | 8.7 ± 4.9 | 4.7 ± 1.6 | 6.1 ± 3.2 | 6.3 ± 2.5 |
| **Accumulation phase** | | | | |
| PHB [%dcw] | 12.5 ± 2 | 14.9 ± 2 | 25.5 ± 8 | 11.7 ± 2 |
| PHB [mg·L$^{-1}$] | 89 ± 16 | 91 ± 22 | 180 ± 76 | 72 ± 18 |
| $\Upsilon_{PHB}$ [mgPHB·L$^{-1}$·d$^{-1}$] | 4.4 ± 3.1 | 6.5 ± 3.9 | 16 ± 11 | 4.9 ± 2.7 |

PHB (Table 1). This consistent synthesis during 168 days represents a significant advancement in cyanobacterial PHB production, exceeding the conventional yields documented in the literature, which typically fall below 10 %dcw PHB in wild-type species in batch experiments no longer than 40 days [2–5,7].

Interestingly, microbiome CW1 surpassed these benchmarks. After 69 days (corresponding to the end of the third repetition), microbiome CW1 distinguished itself, achieving a significant milestone of 37 %dcw PHB, becoming statistically superior ($p < 0.05$) from the other three microbiomes (Fig. 2 and Fig. A.3). This remarkable content was sustained across two successive cycles, specifically from repetitions three to five. Later, the PHB content decreased but remained consistently high for the remainder of the experiment (21–27 %dcw from the sixth to tenth repetition, Fig. 2 and Fig. A.3). On average, this microbiome produced 26 ± 8 %dcw PHB (180 ± 76 mgPHB·L$^{-1}$) during the ten cycles performed (Table 1). This performance was statistically significantly superior ($p < 0.05$) to the other cultures, highlighting CW1's effectiveness in sustaining high PHB production for a long-term period.

Notably, the observed PHB content ranks among the highest values documented for cyanobacteria strains such as *Synechocystis* sp. or *Synechococcus* sp., both identified within CW1. For example, [10] reported a PHB content of 29 %dcw by *Synechocystis* sp. after a 14-day cultivation period under nutrient limitation with a higher acetate addition (4 g·L$^{-1}$). Similarly, the same strain achieved a PHB content of 32 %dcw in five days after acetate addition (4 g·L$^{-1}$) [43]. While these batch studies in small-scale (≤ 100 mL) flasks under sterile conditions achieved impressive PHB yields within short durations (5–14 days), our approach demonstrates a significant advancement by achieving comparable PHB content (26 ± 8 %dcw PHB) under non-sterile conditions in a larger working volume (2.5 L) and, crucially, maintaining long-term production over 168 days. This sustained production over an extended period and in a more scalable, non-sterile environment distinguishes our findings and underscores the potential of this process for continuous PHB accumulation. Following cycles of growth-accumulation phases, a cyanobacteria microbiome primarily dominated by *Synechocystis* sp. achieved comparable PHB content (28 %dcw over 108 days) [25].

### 3.3. Glycogen evolution

Cyanobacteria, when exposed to light, use photosynthesis via the Calvin-Benson-Bassham (CBB) cycle to convert $CO_2$ into organic carbon. This pathway generates carbohydrates, which serve as building blocks for biosynthesis and are stored as glycogen.

During the growth phases, all microbiomes exhibited a consistent increase in glycogen content, reaching substantial levels between 20–50 %dcw glycogen (Fig. 2). Conversely, a pronounced decline in glycogen content was observed across all repetitions and microbiomes during the accumulation phases, a phenomenon likely driven by glycogen catabolism in the dark [44,45]. Specifically, this catabolism resulted in a glycogen reduction of approximately by 10–30 % by the end of each repetition. While the breakdown of glycogen presents a potential internal source of acetyl-CoA, the crucial precursor for PHB synthesis, our findings reveal a more complex relationship than a simple direct conversion. Indeed, the microbiome exhibiting the highest PHB production (CW1) did not had higher glycogen levels. In fact, this microbiome CW1 displayed a lower overall glycogen content compared to the other microbiomes (Fig. 2). This observation aligns with the understanding that acetyl-CoA, generated from glycogen degradation, can be channelled into various metabolic pathways beyond PHB synthesis [46–48]. These alternative pathways, such as fatty acid biosynthesis or the production of other bioproducts like isobutanol or glutamate, likely compete for the available acetyl-CoA, explaining why higher initial glycogen levels do not necessarily translate to increased PHB accumulation. This highlights the intricate regulatory mechanisms within the mixed microbial communities and suggests that maximizing PHB production requires more than simply promoting glycogen accumulation

### 3.4. Acetate consumption

The supplementation of a suitable organic carbon source into the medium increases the availability of acetyl-CoA, possibly enhancing PHB synthesis. While glucose has also been investigated as a potential inducer of PHB synthesis, its effectiveness is generally lower compared to that of acetate [41,49]. For instance, [41] demonstrated that supplementing a culture of cyanobacteria *Synechococcus* sp. with 1 g·L$^{-1}$ of glucose resulted in a PHB concentration of 252.4 mg·L$^{-1}$, whereas the same amount of acetate yielded a significantly higher PHB of 607.2 mg·L$^{-1}$.

Acetate consumption during the accumulation phase differed among the four microbiomes (Fig. 2). Microbiome CW1 generally consumed the initially added 600 mg·L$^{-1}$ in each repetition, with only the first, second, and fifth repetitions showing incomplete consumption (residual acetate > 300 mg·L$^{-1}$). R2 and CW2 exhibited a trend of lower acetate consumption than CW1, leaving residual acetate concentrations between 100 and 400 mg·L$^{-1}$ at the end of the repetitions. Notably, the lowest acetate consumption was observed in microbiome R1, where near-zero consumption was observed in repetitions 1, 3, 4, and 6, leading to high residual acetate levels (> 500 mg·L$^{-1}$).

These distinct acetate consumption profiles correlated with the observed differences in PHB content among the microbiomes (Fig. 2). CW1, exhibiting the highest acetate consumption, also accumulated the most PHB, while the lower acetate consumption observed in R1, R2 and CW2 aligned with their comparatively lower PHB levels.

In addition, the higher glycogen content observed in R1, R2, and CW2 during the growth phase, compared to CW1, may be attributed to the residual acetate. Specifically, at the end of each growth phase, glycogen content in microbiomes R1, R2 and CW2 ranged from 25 to 40 %dcw glycogen, while it was lower in CW1 (around 20 %dcw glycogen) (Fig. 2). It is plausible that during the growth phase, microbiomes R1, R2 and CW2 used the residual acetate as carbon source for biomass growth as well as for carbon storage in the form of glycogen. This phenomena, known as photoheterotrophic metabolism – the assimilation of an organic carbon source in the presence of light – has been previously reported in cyanobacteria [49–51].

### 3.5. Expression of key genes involved in PHB and glycogen metabolism

The good performance of microbiome CW1 in biopolymer synthesis was reflected at gene expression level. Notably, results revealed that only microbiome CW1 displayed a statically significant ($p < 0.05$) overexpression of gene *phaC* (encoding poly(3-hydroxyalkanoate) synthase) by day seven of the accumulation phase from repetition 3 (corresponding to day 69 of the entire experiment). This overexpression was

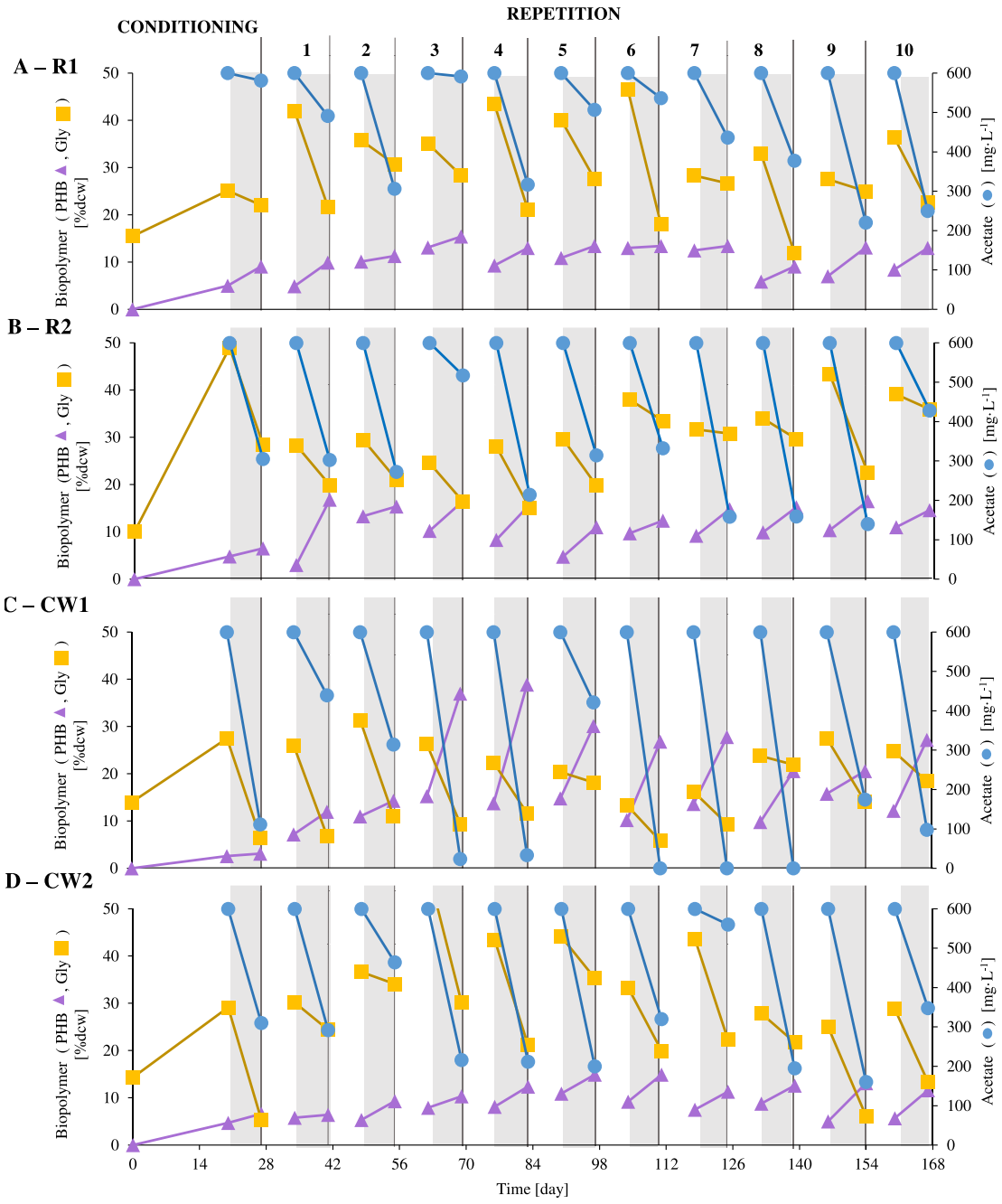


**Fig. 2.** Evolution of biopolymers (PHB and glycogen) and acetate concentration for microbiomes (A) R1; (B) R2; (C) CW1; and (D) CW2. Three measurements were done at each cycle: in the beginning of the growth phase, the beginning of the accumulation phase and the end of the accumulation phase. The white areas correspond to the growth phase. The onset of the accumulation phase in each cycle is marked by dashed vertical lines, with the grey area highlighting the duration of this phase. The completion of the cycle is indicated by solid vertical black lines.

nearly six-fold higher compared to the initial time (Fig. 3B).

Furthermore, on day 69, both CW1 and CW2 exhibited overexpression of genes associated with glycogen catabolism (*glgP1* and *glgP2*, which encode for glycogen phosphorylase) compared to the inoculum (Fig. 3B and C). This upregulation aligns with the observed glycogen degradation during the starvation phases (Fig. 2). This catabolic activity would lead to an elevated pool of acetyl-CoA, the crucial precursor for PHB biosynthesis [25,52,53], potentially enhancing PHB accumulation. Interestingly, the specific *glgP* gene upregulated differed between the two microbiomes: *glgP1* expression was higher in CW1, while *glgP2* showed increased levels in CW2. While [53] suggested that *glgP2*-mediated glycogen catabolism is essential for sustained PHB synthesis under prolonged nitrogen starvation, our results contradict this, as CW2, with higher *glgP2* expression, accumulated less PHB than CW1. Notably, our finding of *glgP1* overexpression correlating with higher PHB production in CW1 aligns with observations in another cyanobacteria-enriched microbiome that achieved up to 28 %dcw PHB [25]. In contrast, in a *Synechocystis* sp. monoculture, *glgP2* was overexpressed in the culture with the highest PHB content [37], suggesting a complex interaction between these genes in the microbiomes.

Consistent with the observed upregulation of glycogen catabolism genes, no overexpression of *glgA* (encoding glycogen synthase) was detected (Fig. 3B and C). This observation further supports the role of glycogen as the primary storage carbohydrate, which, upon prolonged

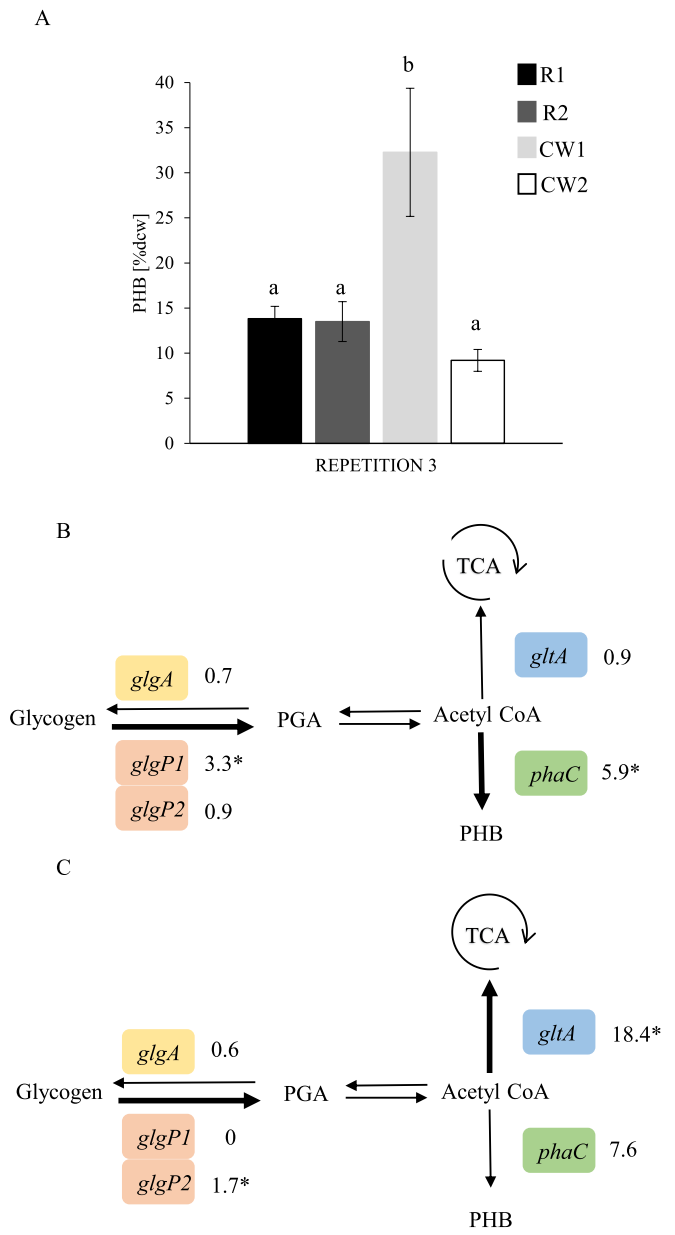


**Fig. 3.** (A) Mean PHB content of the four microbiomes in repetition 3 (day 69). Error lines indicate the standard deviation of the measurements. The microbiome labeled with a different letter (CW1) is significantly different in terms of mean PHB content (Tukey test). (B and C) Schematic representation of biosynthesis pathways for PHB and glycogen production in cyanobacteria with the results from gene expression analysis on day 69 for microbiome (B) CW1, and (C) CW2. The genes evaluated are shown inside rectangles, with numbers next to the rectangles indicating the level of gene expression as fold changes. Day 0 is used as a reference value. Thicker arrows indicate an overexpression of that metabolic route. Statistically significant overexpressed genes are marked with an asterisk (*), denoting a $p$-value $< 0.05$. Key genes are color-coded: yellow for glycogen synthesis (*glgA*); orange, for glycogen catabolism (*glgP1*, *glgP2*); green for synthesis of PHB (*phaC*); and blue for acetyl-CoA entry into the tricarboxylic acid (TCA) cycle (*gltA*). Abbreviations: *glgA*: glycogen synthase; *glgP1* and *glgP2*: glycogen phosphorylase; *gltA*: citrate synthase; PGA: 3-phosphoglycerate; *phaC*: poly(3-hydroxyalkanoate) synthase. (For interpretation of the references to color in this figure legend, the reader is referred to the web version of this article.)

nutrient deprivation, is catabolized to provide carbon for PHB synthesis or other metabolic pathways [52,53]. Indeed, prior research involving cyanobacterial microbiomes has indicated that *glgA* overexpression, associated with glycogen synthesis, occurs during the initial days of the accumulation phase, but this upregulation is absent after seven days of starvation [25]. These findings highlight the importance of glycogen storage during the growth phase; suggesting that sufficient inorganic carbon availability is essential for synthetizing the glycogen reserves that can subsequently converted into PHB, ultimately contributing to high PHB content. Therefore, ensuring sufficient inorganic carbon availability during the growth phase appears to be a key factor in maximising PHB synthesis potential. However, the findings of [37] on *Synechocystis* sp. underscore the importance of additional factors beyond inorganic carbon concentration for achieving high PHB content. Their evaluation across a range of bicarbonate concentrations (as bicarbonate, 0–2 $g{\cdot}L^{-1}$) revelead that even at the highest concentration (2 $g{\cdot}L^{-1}$), PHB content did not exceed 14 %dcw. This limited accumulation was likely due to the continuous light exposure during the accumulation phase and the absence of acetate supplementation. This suggests that while sufficient inorganic carbon during the growth phase is a prerequisite for building the necessary glycogen reserves, the presence of exogenous organic carbon source like acetate and a dark environment are also crucial to enhance biopolymer accumulation.

By day 69, gene *gltA*, which is linked to the TCA cycle, demonstrated significant overexpression in microbiome CW2. Its expression level increased 18 times that of the inoculum (Fig. 3C). In contrast, in culture CW1, the same gene did not exhibit any significant overexpression, highlighting a stark contrast between the two cultures regarding carbon flux. This difference in gene expression was clearly reflected on the distinctive PHB accumulation of each microbiome. The discrepancy suggested that in CW2 a significant portion of the acetyl-CoA was directed towards the TCA cycle rather than being channelled into PHB synthesis. This potential metabolic redirection could indeed explain the lower levels of PHB yield observed in CW2 (10 %dcw) compared to the significantly higher yield in CW1 (37 %dcw). Considering this scenario, employing labelled carbon sources, such as $^{13}$C-bicarbonate or $^{13}$C-acetate, can help elucidating the distribution of acetyl-CoA within the metabolic pathways and the precise distribution of carbon [54,55]. This approach would allow for a more detailed understanding of how carbon is allocated between different metabolic routes and help clarify the differences in PHB production observed between microbiomes, thereby optimizing strategies to increase biopolymer production.

### 3.6. Microbial composition analysis

The analysis of gene amplicon sequences targeting the bacterial 16S rRNA gene variable regions 1–3 enabled us to estimate the relative abundance of various microbial groups in each microbiome throughout the study. Abundance data obtained from these analyses is shown in the Supplementary Material.

The dynamics of microbial community composition at the class level in microbiomes CW1 (representative of high PHB producer) and CW2 (representative of low PHB producer) are shown in Fig. 4A, covering from the initial stage of the experiment (day 1) to the beginning of the accumulation phase in the tenth repetition (day 160). Cyanobacteria usually dominated the microbiomes with relative abundances generally higher than 50 %. Within the Cyanobacteria, the genera *Synechocystis* and *Synechococcus* were identified in both CW1 and CW2 (Fig. 4B). Notably, *Synechocystis* maintained its dominance across all experimental repetitions, with no statistically significant differences observed in its relative abundance among the four microbiomes (Fig. A.4). This consistent dominance suggests a key role for *Synechocystis* in the phototrophic microbiomes under study. A major distinction among the cultures was the presence of Alphaproteobacteria, detected in both CW1 and CW2 but exhibiting variable relative abundances depending on the specific microbiome and experimental phase. Within the

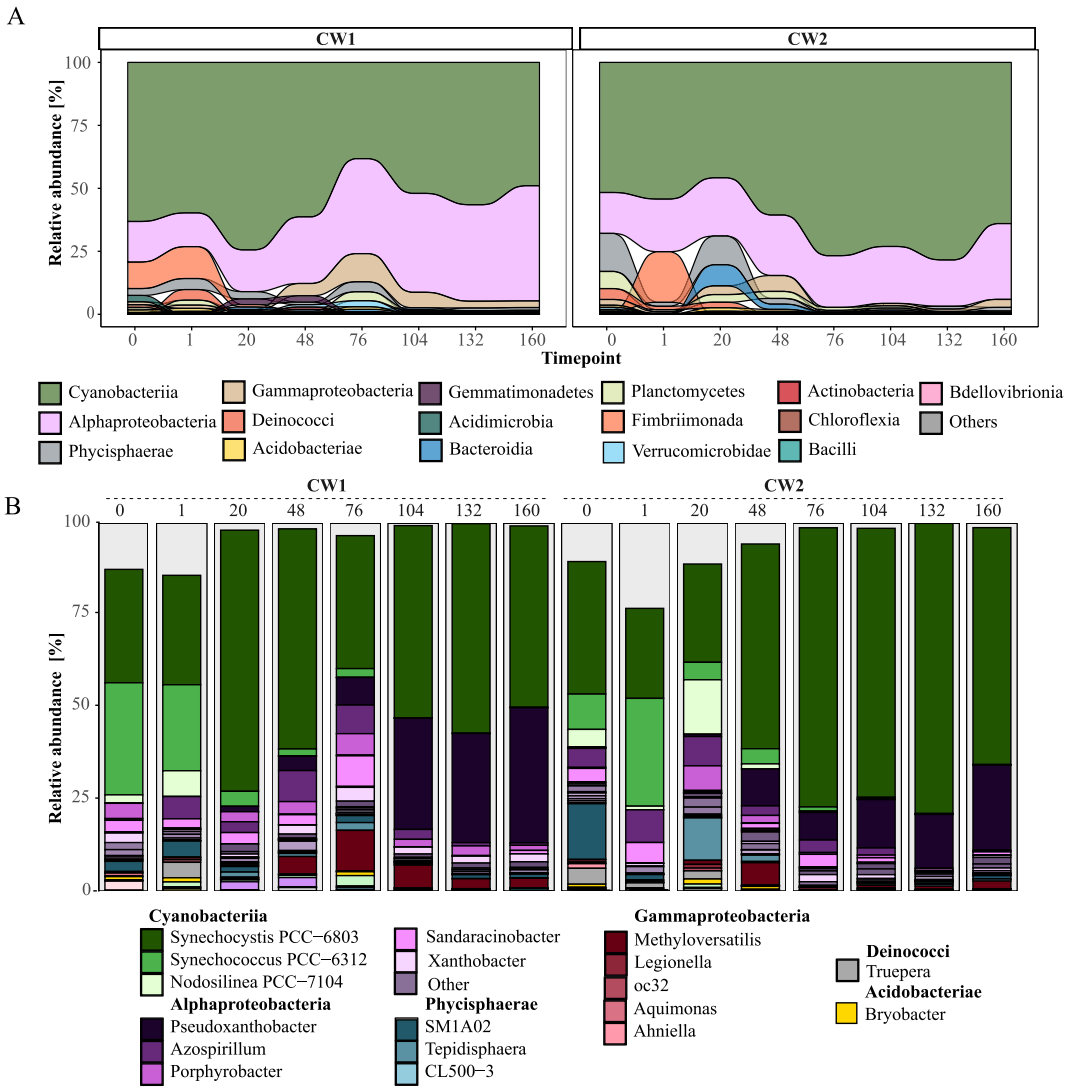


**Fig. 4.** Relative abundances of microbial taxa at the (A) class and (B) genus level in the CW1 and CW2 microbiomes, from the start of the experiment (day 0) until day 160 (the beginning of the accumulation phase from repetition 10). To simplify the figure, only the genera with more than 1% of abundance are included. Specifically, for Alphaproteobacteria in panel (B), the five most abundant taxa are displayed, while the remainder are grouped as "Other".

Alphaproteobacteria class, the predominant genera were *Pseudoxanthomonas* and *Azospirillum*, both of which contain species known for their nitrogen-fixing capabilities [56,57].

In microbiome CW1, Alphaproteobacteria abundance rose around repetition 3 and 4 (days 48 and 76). This increase corresponded with the peak in PHB content, reaching 37 %dcw PHB on day 69 (Fig. 2). After repetition 4, the relative abundance of Alphaproteobacteria and of Cyanobacteria stabilized at nearly equal relative abundances (slightly less than 50 % each). This period corresponded with the final repetitions, during which microbiome CW1 consistently achieved PHB content of around 21–27 %dcw. In contrast, in microbiome CW2, on the same repetitions, the relative abundance of Cyanobacteria and Alphaproteobacteria shifts from a balanced state to a significant increase in Cyanobacteria compared to Alphaproteobacteria (75 % vs. 20 %) (Fig. 4 and Fig. A.4). These findings suggest that the relationship between these two groups may play a crucial role in maintaining high PHB production. The fundamental mechanisms underlying this relationship remain unclear, but several possibilities could explain this dynamic. For instance, Cyanobacteria may supply organic carbon or other metabolites that support Alphaproteobacteria growth, fostering a mutually beneficial environment that promotes stable PHB production [58]. Further investigations, such as metabolic flux analysis and transcriptomic studies, are needed to clarify the specific interactions driving this synergy and their impact on PHB accumulation.

To the authors' knowledge, the analysis of microbiome composition from cyanobacteria-enriched microbiomes has not been previously characterized, limiting the opportunity for direct comparison with existing literature. However, [59] investigated the impact of varying operational conditions on bacterial communities within a phototrophic microbiome enriched with purple phototrophic bacteria. They identified members of the the *Chromatiaceae* family (purple bacteria) as the dominant phototrophic PHA producers, alongside Alphaproteobacteria, including the genera *Rhodopseudomonas*, *Rhodobacter*, and *Rhizobium*. Their findings suggest that in a feast-famine operational system, an extended feast phase or higher organic loading rate is necessary to obtain a microbiome more enriched in phototrophic purple bacteria. These conditions favour the growth of *Rhodopseudomonas*, *Rhizobium*, and Hyphomicrobiaceae, leading to the presence of *Rhodobacter* and Chromatiaceae, and resulting in a community capable of high PHA productivities. In contrast, in our cyanobacteria-dominated system, Alphaproteobacteria were also detected, but the predominant genera differed. Specifically, we observed higher relative abundances of *Pseudoxanthobacter*, *Azospirillum*, *Sandaracinobacter*, and *Roseococcus*, among others (Fig. 4B). It is important to note that despite the presence of

Alphaproteobacteria, Cyanobacteria were the primary PHB accumulators, as confirmed by Nile Blue staining (Fig. 5). This highlights a key distinction in PHA production strategies between purple bacteria-dominated and cyanobacteria-dominated phototrophic cultures, where in the latter, PHB accumulation is primarily exclusive to the cyanobacteria population.

### 3.7. Visualization of PHB granules by confocal laser microscopy

Microscopic analysis conducted at the experiment's conclusion on day 168 revealed the presence of PHB granules in all four microbiomes (Fig. 5). In fact, the PHB content in each microbiome at this time point exceeded 5 %dcw, the minimum threshold for effective microscopic detection [7]. A significant observation was the considerable heterogeneity in the intracellular distribution of the biopolymer. While some cells displayed a high density of PHB granules, indicative of substantial accumulation, others showed no discernible evidence of PHB storage. This cellular variability in PHB accumulation could be attributed to the differential expression of key enzymes involved in PHB synthesis pathway, such as PhaC [60], leading to a spectrum of PHB granule numbers per cell. This phenotypic variation in biopolymer formation is a phenomenon documented in previous studies across both pure and mixed cultures of cyanobacteria, as well as in mixed cultures of heterotrophic bacteria [25,60–63].

## 4. Conclusions

In this study, four cyanobacteria-rich microbiomes were evaluated in terms of PHB synthesis over 168 days. Despite applying consistent environmental and cultivation conditions to the cultures, significant differences in biopolymer accumulation were observed, highlighting the influence of microbial community on PHB production. By overlapping PHB quantification data, DNA sequencing and RT-qPCR data, links between PHB content, microbial community, and gene expression could be detected. The high PHB content in CW1 microbiome was associated with upregulation of the *phaC* gene, involved in PHB synthesis, and *glgp1*, linked to glycogen catabolism. This suggested an interaction between PHB and glycogen pathways that supports higher PHB accumulation. In contrast, lower PHB production in CW2 microbiome (a representative example of microbiome with reduced PHB content) correlated with the overexpression of *gltA*, a gene involved in the TCA cycle, which may divert metabolic resources away from PHB synthesis. Moreover, variations in the relative abundance of Cyanobacteria and Alphaproteobacteria were observed across microbiomes. The stabilization of Alphaproteobacteria and Cyanobacteria relative abundances in CW1 were associated to high PHB content. The findings suggest that maintaining a balanced coexistence between these microbial groups may be critical for achieving optimal PHB production in cyanobacteria-enriched microbiomes. However, it is important to note that the specific mechanisms underlying this interaction remain unclear and further

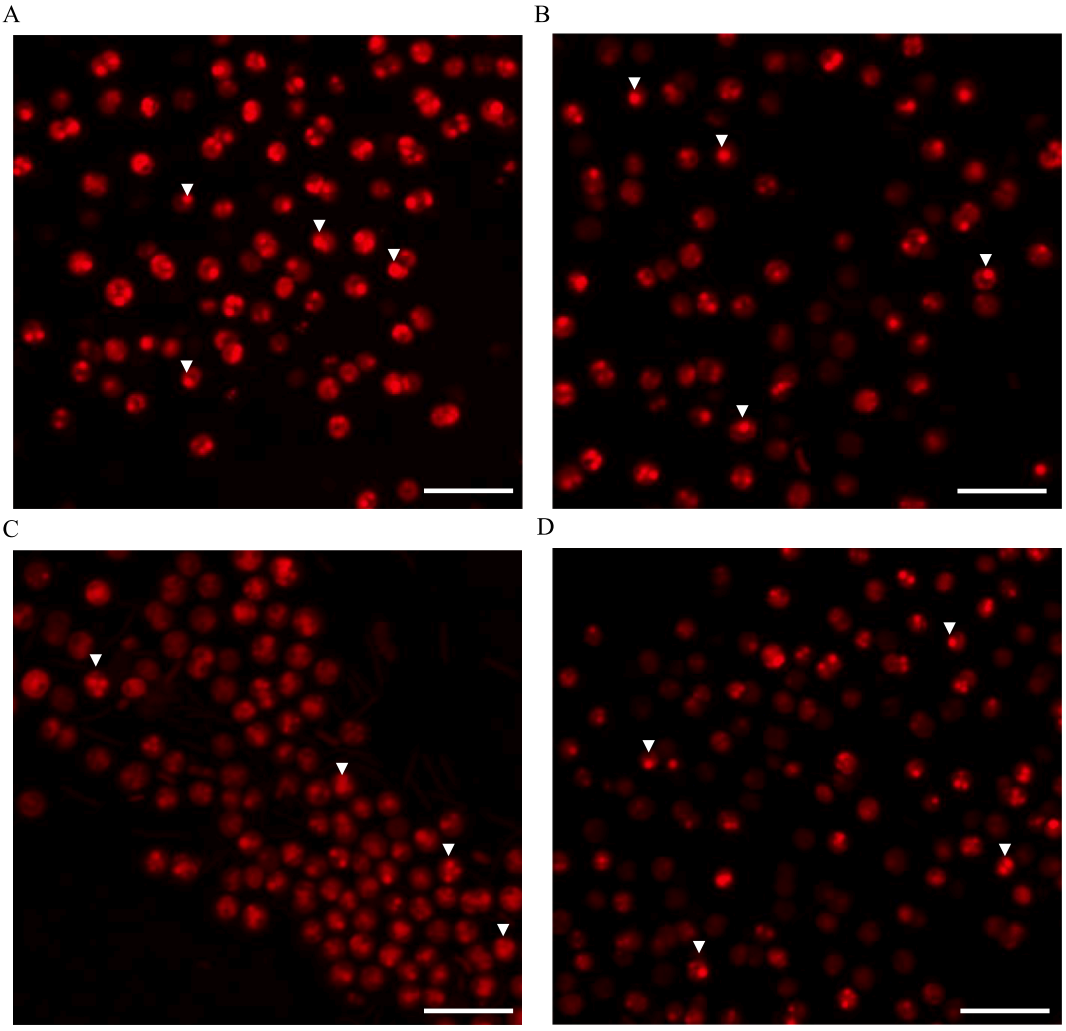


**Fig. 5.** Confocal laser scanning microscope images of microbiomes (A) R1; (B) R2; (C) CW1; and (D) CW2 by the end of repetition 10 (day 168 of the whole experiment). PHB granules are clearly detected as dots within the cells. White arrow heads point to some of the PHB granules. Scale bar is 10 μm.

investigation is needed to elucidate the precise roles of each microbial group in PHB accumulation.

## CRediT authorship contribution statement

**Beatriz Altamira-Algarra:** Writing – original draft, Investigation, Conceptualization. **Lin Sun:** Investigation. **David San León Granado:** Writing – review & editing, Investigation. **Lucía Romero-Morillo:** Investigation. **Livia Vurro:** Investigation. **Juan Nogales:** Writing – review & editing. **Eva Gonzalez-Flo:** Writing – review & editing, Supervision, Conceptualization. **Joan Garcia:** Writing – review & editing, Supervision, Project administration, Funding acquisition, Conceptualization.

## Declaration of competing interest

The authors declare that they have no known competing financial interests or personal relationships that could have appeared to influence the work reported in this paper.

## Acknowledgements

This work was supported by the European Union's Horizon 2020 research and innovation programme under the grant agreement No 101000733 (project PROMICON). B.A.A. acknowledges the Agency for Management of University and Research (AGAUR) for her grant [FIA-GAUR_2021]. L.S. thanks the financial support from the program of China Scholarships Council (No. 202308440158) J. N. acknowledges the support of SyCoSys project, TED2021-130689B-C33 funded by MCIN/AEI/10.13039/ 501100011033 and the European Union "NextGenerationEU"/PRTR. E.G.F. would like to thank the European Union-NextGenerationEU, Ministry of Universities and Recovery, Transformation and Resilience Plan for her research grant [2021UPF-MS-12]. J.G. acknowledges the support provided by the ICREA Academia program. The authors would like to sincerely thank ADM Biopolis (València, Spain) for their assistance in performing the 16S rRNA gene amplification, and the Barcelona Research Center in Multiscale Science and Engineering (Barcelona, Spain) for their support with the confocal laser scanning microscopy.

## Appendix A. Supplementary data

Supplementary data to this article can be found online at https://doi.org/10.1016/j.cej.2025.164196.

## Data availability

Data will be made available on request.

## References

[1] H. Park, H. He, X. Yan, X. Liu, N.S. Scrutton, G.Q. Chen, PHA is not just a bioplastic!, Biotechnol. Adv. 71 (2024), https://doi.org/10.1016/j.biotechadv.2024.108320.
[2] S. Ansari, T. Fatma, Cyanobacterial polyhydroxybutyrate (PHB): Screening, optimization and characterization, PLoS One 11 (2016) 1–20, https://doi.org/10.1371/journal.pone.0158168.
[3] T. Monshupanee, A. Incharoensakdi, Enhanced accumulation of glycogen, lipids and polyhydroxybutyrate under optimal nutrients and light intensities in the cyanobacterium Synechocystis sp. PCC 6803, J. Appl. Microbiol. 116 (2014) 830–838, https://doi.org/10.1111/jam.12409.
[4] E. Rueda, E. Gonzalez-Flo, L. Roca, J. Carretero, J. Garciá, Accumulation of polyhydroxybutyrate in Synechocystis sp. isolated from wastewaters: Effect of salinity, light, and P content in the biomass, J. Environ. Chem. Eng. 10 (2022) 107952, https://doi.org/10.1016/j.jece.2022.107952.
[5] E. Rueda, M.J. García-Galán, R. Díez-Montero, J. Vila, M. Grifoll, J. García, Polyhydroxybutyrate and glycogen production in photobioreactors inoculated with wastewater borne cyanobacteria monocultures, Bioresour. Technol. 295 (2020) 122233, https://doi.org/10.1016/j.biortech.2019.122233.
[6] D. Kamravamanesh, S. Pflügl, W. Nischkauer, A. Limbeck, M. Lackner, C. Herwig, Photosynthetic poly-β-hydroxybutyrate accumulation in unicellular cyanobacterium Synechocystis sp. PCC 6714, AMB Express 7 (2017), https://doi.org/10.1186/s13568-017-0443-9.
[7] K. Sudesh, K. Taguchi, Y. Doi, Effect of increased PHA synthase activity on polyhydroxyalkanoates biosynthesis in Synechocystis sp. PCC6803, Int. J. Biol. Macromol. 30 (2002) 97–104, https://doi.org/10.1016/S0141-8130(02)00010-7.
[8] E. Rueda, B. Altamira-Algarra, J. García, Process optimization of the polyhydroxybutyrate production in the cyanobacteria Synechocystis sp. and Synechococcus sp, Bioresour. Technol. 356 (2022) 127330, https://doi.org/10.1016/J.BIORTECH.2022.127330.
[9] S. Tanweer, B. Panda, Prospect of Synechocystis sp. PCC 6803 for synthesis of poly (3-hydroxybutyrate-co-4-hydroxybutyrate), Algal Res. 50 (2020) 101994, https://doi.org/10.1016/j.algal.2020.101994.
[10] B. Panda, P. Jain, L. Sharma, N. Mallick, Optimization of cultural and nutritional conditions for accumulation of poly-β-hydroxybutyrate in Synechocystis sp. PCC 6803, Bioresour. Technol. 97 (2006) 1296–1301, https://doi.org/10.1016/j.biortech.2005.05.013.
[11] B. Panda, N. Mallick, Enhanced poly-b-hydroxybutyrate accumulation in a unicellular cyanobacterium, Synechocystis sp. PCC 6803, Lett. Appl. Microbiol. 44 (2007) 194–198, https://doi.org/10.1111/j.1472-765X.2006.02048.x.
[12] Z. Zahra, D.H. Choo, H. Lee, A. Parveen, Cyanobacteria: review of current potentials and applications, Environ. - MDPI 7 (2020), https://doi.org/10.3390/environments7020013.
[13] M. Baunach, A. Guljamow, M. Miguel-Gordo, E. Dittmann, Harnessing the potential: advances in cyanobacterial natural product research and biotechnology, Nat. Prod. Rep. 41 (2023) 347–369, https://doi.org/10.1039/d3np00045a.
[14] D. Chittora, M. Meena, T. Barupal, P. Swapnil, Cyanobacteria as a source of biofertilizers for sustainable agriculture, Biochem. Biophys. Reports 22 (2020) 100737, https://doi.org/10.1016/j.bbrep.2020.100737.
[15] W. Khetkorn, A. Incharoensakdi, P. Lindblad, S. Jantaro, Enhancement of poly-3-hydroxybutyrate production in Synechocystis sp. PCC 6803 by overexpression of its native biosynthetic genes, Bioresour. Technol. 214 (2016) 761–768, https://doi.org/10.1016/j.biortech.2016.05.014.
[16] C. Troschl, K. Meixner, I. Fritz, K. Leitner, A.P. Romero, A. Kovalcik, P. Sedlacek, B. Drosg, Pilot-scale production of poly-β-hydroxybutyrate with the cyanobacterium Synechocytis sp. CCALA192 in a non-sterile tubular photobioreactor, Algal Res. 34 (2018) 116–125, https://doi.org/10.1016/j.algal.2018.07.011.
[17] M. Mariotto, S. Egloff, I. Fritz, D. Refardt, Cultivation of the PHB-producing cyanobacterium Synechococcus leopoliensis in a pilot-scale open system using nitrogen from waste streams, Algal Res. 70 (2023) 103013, https://doi.org/10.1016/j.algal.2023.103013.
[18] E. Rueda, M.J. García-Galán, A. Ortiz, E. Uggetti, J. Carretero, J. García, R. Díez-Montero, Bioremediation of agricultural runoff and biopolymers production from cyanobacteria cultured in demonstrative full-scale photobioreactors, Process Saf. Environ. Prot. 139 (2020) 241–250, https://doi.org/10.1016/j.psep.2020.03.035.
[19] D. Kamravamanesh, D. Kiesenhofer, S. Fluch, M. Lackner, C. Herwig, Scale-up challenges and requirement of technology-transfer for cyanobacterial poly (3-hydroxybutyrate) production in industrial scale, Int. J. Biobased Plast. 1 (2019) 60–71, https://doi.org/10.1080/24759651.2019.1688604.
[20] V. Senatore, E. Rueda, M. Bellver, R. Díez-Montero, I. Ferrer, T. Zarra, V. Naddeo, J. García, Production of phycobiliproteins, bioplastics and lipids by the cyanobacteria Synechocystis sp. treating secondary effluent in a biorefinery approach, Sci. Total Environ. 857 (2023), https://doi.org/10.1016/j.scitotenv.2022.159343.
[21] Á. Estévez-Alonso, B. Altamira-Algarra, C. Arnau-Segarra, M.C.M. van Loosdrecht, R. Kleerebezem, A. Werker, Process conditions affect properties and outcomes of polyhydroxyalkanoate accumulation in municipal activated sludge, Bioresour. Technol. 364 (2022), https://doi.org/10.1016/j.biortech.2022.128035.
[22] L. Wang, Y.W. Cui, Simultaneous treatment of epichlorohydrin wastewater and polyhydroxyalkanoate recovery by halophilic aerobic granular sludge highly enriched by Halomonas sp, Bioresour. Technol. 391 (2024), https://doi.org/10.1016/j.biortech.2023.129951.
[23] J.R. Almeida, M.A. Miranda Reis, J.C. Fradinho, Influence of inorganic carbon on purple phototrophic bacteria polyhydroxyalkanoates production under high reductive stress environment, Bioresour. Technol. 428 (2025), https://doi.org/10.1016/j.biortech.2025.132462.
[24] B. Altamira-Algarra, J. Garcia, E. Gonzalez-Flo, Cyanobacteria microbiomes for bioplastic production: Critical review of key factors and challenges in scaling from laboratory to industry set-ups, Bioresour. Technol. 422 (2025) 132231, https://doi.org/10.1016/j.biortech.2025.132231.
[25] B. Altamira-Algarra, A. Lage, A.L. Meléndez, M. Arnau, E. Gonzalez-Flo, J. García, Bioplastic production by harnessing cyanobacteria-rich microbiomes for long-term synthesis, Sci. Total Environ. 954 (2024) 1–15, https://doi.org/10.1016/j.scitotenv.2024.176136.
[26] B. Altamira-Algarra, E. Rueda, A. Lage, D. San León, J.F. Martínez-Blanch, J. Nogales, J. García, E. Gonzalez-Flo, New strategy for bioplastic and exopolysaccharides production: Enrichment of field microbiomes with cyanobacteria, N, Biotechnol. 78 (2023) 141–149, https://doi.org/10.1016/j.nbt.2023.10.008.
[27] E. Gonzalez-Flo, X. Romero, J. García, Nature based-solutions for water reuse: 20 years of performance evaluation of a full-scale constructed wetland system, Ecol. Eng. 188 (2023) 106876, https://doi.org/10.1016/j.ecoleng.2022.106876.
[28] B. Altamira-Algarra, A. Lage, J. Garcia, E. Gonzalez-Flo, Photosynthetic species composition determines bioplastics production in microbiomes: strategy to enrich

cyanobacteria PHB-producers, Algal Res. 79 (2024), https://doi.org/10.1016/j.algal.2024.103469.
[29] American Public Health Association, Standard Methods for the Examination of Water and Wastewater, 22nd ed., 2012.
[30] A.B. Lanham, A.R. Ricardo, M.G.E. Albuquerque, F. Pardelha, M. Carvalheira, M. Coma, J. Fradinho, G. Carvalho, A. Oehmen, M.A.M. Reis, Determination of the extraction kinetics for the quantification of polyhydroxyalkanoate monomers in mixed microbial systems, Process Biochem. 48 (2013) 1626–1634, https://doi.org/10.1016/j.procbio.2013.07.023.
[31] A.B. Lanham, A.R. Ricardo, M. Coma, J. Fradinho, M. Carvalheira, A. Oehmen, G. Carvalho, M.A.M. Reis, Optimisation of glycogen quantification in mixed microbial cultures, Bioresour. Technol. 118 (2012) 518–525, https://doi.org/10.1016/j.biortech.2012.05.087.
[32] S. Yuan, D.B. Cohen, J. Ravel, Z. Abdo, L.J. Forney, Evaluation of methods for the extraction and purification of DNA from the human microbiome, PLoS One 7 (2012), https://doi.org/10.1371/journal.pone.0033865.
[33] A. Klindworth, E. Pruesse, T. Schweer, J. Rg Peplies, C. Quast, M. Horn, F.o., Glö Ckner, Evaluation of general 16S ribosomal RNA gene PCR primers for classical and next-generation sequencing-based diversity studies, Nucleic Acids Res. 41 (2013), https://doi.org/10.1093/nar/gks808.
[34] D.E. Wood, J. Lu, B. Langmead, Improved metagenomic analysis with Kraken 2, Genome Biol. 20 (2019) 1–13, https://doi.org/10.1186/s13059-019-1891-0.
[35] D. Straub, N. Blackwell, A. Langarica-Fuentes, A. Peltzer, S. Nahnsen, S. Kleindienst, Interpretations of environmental microbial community studies are biased by the selected 16S rRNA (Gene) amplicon sequencing pipeline, Front. Microbiol. 11 (2020) 1–18, https://doi.org/10.3389/fmicb.2020.550420.
[36] C. Liu, Y. Cui, X. Li, M. Yao, Microeco: An R package for data mining in microbial community ecology, FEMS Microbiol. Ecol. 97 (2021) 1–9, https://doi.org/10.1093/femsec/fiaa255.
[37] E. Rueda, A. Álvarez-González, J. Vila, R. Díez-Montero, M. Grifoll, J. García, Inorganic carbon stimulates the metabolic routes related to the polyhdroxybutyrate production in a Synechocystis sp. strain (cyanobacteria) isolated from wastewater, Sci. Total Environ. 829 (2022), https://doi.org/10.1016/j.scitotenv.2022.154691.
[38] S.A. Bustin, V. Benes, J.A. Garson, J. Hellemans, J. Huggett, M. Kubista, R. Mueller, T. Nolan, M.W. Pfaffl, G.L. Shipley, J. Vandesompele, C.T. Wittwer, The MIQE guidelines: Minimum information for publication of quantitative real-time PCR experiments, Clin. Chem. 55 (2009) 611–622, https://doi.org/10.1373/clinchem.2008.112797.
[39] D.M. Arias, E. Rueda, M.J. García-Galán, E. Uggetti, J. García, Selection of cyanobacteria over green algae in a photo-sequencing batch bioreactor fed with wastewater, Sci. Total Environ. 653 (2019) 485–495, https://doi.org/10.1016/j.scitotenv.2018.10.342.
[40] D.M. Arias, E. Uggetti, M.J. García-Galán, J. García, Nutrients and biomass dynamics in photo-sequencing batch reactors treating wastewater with high nutrients loadings, Ecol. Eng. 119 (2018) 35–44, https://doi.org/10.1016/j.ecoleng.2018.05.016.
[41] S.Y. Lee, J.S. Lee, S.J. Sim, Cost-effective production of bioplastic polyhydroxybutyrate via introducing heterogeneous constitutive promoter and elevating acetyl-Coenzyme A pool of rapidly growing cyanobacteria, Bioresour. Technol. 394 (2024) 130297, https://doi.org/10.1016/j.biortech.2023.130297.
[42] C. Troschl, K. Meixner, B. Drosg, Cyanobacterial PHA production—review of recent advances and a summary of three years' working experience running a pilot plant, Bioengineering 4 (2017) 26, https://doi.org/10.3390/bioengineering4020026.
[43] L.H. Gracioso, A. Bellan, B. Karolski, L.O.B. Cardoso, E.A. Perpetuo, C.A.O. do Nascimento, R. Giudici, V. Pizzocchero, M. Basaglia, T. Morosinotto, Light excess stimulates Poly-beta-hydroxybutyrate yield in a mangrove-isolated strain of Synechocystis sp, Bioresour. Technol. 320 (2021) 1–7, https://doi.org/10.1016/j.biortech.2020.124379.
[44] A. Makowka, L. Nichelmann, D. Schulze, K. Spengler, C. Wittmann, K. Forchhammer, K. Gutekunst, Glycolytic shunts replenish the Calvin–Benson–Bassham cycle as anaplerotic reactions in cyanobacteria, Mol. Plant 13 (2020) 471–482, https://doi.org/10.1016/j.molp.2020.02.002.
[45] R. Saha, D. Liu, A. Hoynes-O'Connor, M. Liberton, J. Yu, M. Bhattacharyya-Pakrasi, A. Balassy, F. Zhang, T.S. Moon, C.D. Maranas, H.B. Pakrasia, Diurnal regulation of cellular processes in the cyanobacterium Synechocystis sp. strain PCC 6803: Insights from transcriptomic, fluxomic, and physiological analyses, Am. Soc. Microbiol. 7 (2016), https://doi.org/10.1128/mBio.00464-16.
[46] M. Ciebiada, K. Kubiak, M. Daroch, Modifying the cyanobacterial metabolism as a key to efficient biopolymer production in photosynthetic microorganisms, Int. J. Mol. Sci. 21 (2020) 1–24, https://doi.org/10.3390/ijms21197204.
[47] X. Li, C.R. Shen, J.C. Liao, Isobutanol production as an alternative metabolic sink to rescue the growth deficiency of the glycogen mutant of Synechococcus elongatus PCC 7942, Photosynth. Res. 120 (2014) 301–310, https://doi.org/10.1007/s11120-014-9987-6.
[48] Y. Kato, R. Hidese, M. Matsuda, R. Ohbayashi, H. Ashida, A. Kondo, T. Hasunuma, Glycogen deficiency enhances carbon partitioning into glutamate for an alternative extracellular metabolic sink in cyanobacteria, Commun. Biol. 7 (2024) 3–11, https://doi.org/10.1038/s42003-024-05929-9.
[49] R. Yan, D. Zhu, Z. Zhang, Q. Zeng, J. Chu, Carbon metabolism and energy conversion of Synechococcus sp. PCC 7942 under mixotrophic conditions: Comparison with photoautotrophic condition, J. Appl. Phycol. 24 (2012) 657–668, https://doi.org/10.1007/s10811-011-9683-2.
[50] C. Duangsri, N.A. Mudtham, A. Incharoensakdi, W. Raksajit, Enhanced polyhydroxybutyrate (PHB) accumulation in heterotrophically grown Arthrospira platensis under nitrogen deprivation, J. Appl. Phycol. 32 (2020) 3645–3654, https://doi.org/10.1007/s10811-020-02272-4.
[51] H. Yu, S. Jia, Y. Dai, Growth characteristics of the cyanobacterium Nostoc flagelliforme in photoautotrophic, mixotrophic and heterotrophic cultivation, J. Appl. Phycol. 21 (2009) 127–133, https://doi.org/10.1007/s10811-008-9341-5.
[52] R. Damrow, I. Maldener, Y. Zilliges, The multiple functions of common microbial carbon polymers, glycogen and PHB, during stress responses in the non-diazotrophic cyanobacterium Synechocystis sp. PCC 6803, Front. Microbiol. 7 (2016) 1–10, https://doi.org/10.3389/fmicb.2016.00966.
[53] M. Koch, S. Doello, K. Gutekunst, K. Forchhammer, PHB is produced from glycogen turn-over during nitrogen starvation in Synechocystis sp. PCC 6803, Int. J. Mol. Sci. 20 (2019), https://doi.org/10.3390/ijms20081942.
[54] V. Dutt, S. Srivastava, Novel quantitative insights into carbon sources for synthesis of poly hydroxybutyrate in Synechocystis PCC 6803, Photosynth. Res. 136 (2018) 303–314, https://doi.org/10.1007/s11120-017-0464-x.
[55] Y. Doi, M. Kunioka, Y. Nakamura, K. Soga, Biosynthesis of copolyesters in Alcaligenes eutrophus H16 from13C-labeled acetate and propionate, Macromolecules 20 (1987) 2988–2991, https://doi.org/10.1021/ma00178a006.
[56] O. Steenhoudt, J. Vanderleyden, Azospirillum, a free-living nitrogen-fixing bacterium closely associated with grasses: Genetic, biochemical and ecological aspects, FEMS Microbiol. Rev. 24 (2000) 487–506, https://doi.org/10.1016/S0168-6445(00)00036-X.
[57] A.B. Arun, P. Schumann, H.I. Chu, C.C. Tan, W.M. Chen, W.A. Lai, P. Kämpfer, F. T. Shen, P.D. Rekha, M.H. Hung, J.H. Chou, C.C. Young, Pseudoxanthobacter soli gen. nov., sp. nov., a nitrogen-fixing alphaproteobacterium isolated from soil, Int. J. Syst. Evol. Microbiol. 58 (2008) 1571–1575, https://doi.org/10.1099/ijs.0.65206-0.
[58] C.M. Zhu, J.Y. Zhang, R. Guan, L. Hale, N. Chen, M. Li, Z.H. Lu, Q.Y. Ge, Y.F. Yang, J.Z. Zhou, T. Chen, Alternate succession of aggregate-forming cyanobacterial genera correlated with their attached bacteria by co-pathways, Sci. Total Environ. 688 (2019) 867–879, https://doi.org/10.1016/j.scitotenv.2019.06.150.
[59] J.R. Almeida, J.C. Fradinho, G. Carvalho, A. Oehmen, M.A.M. Reis, Dynamics of microbial communities in phototrophic polyhydroxyalkanoate accumulating cultures, Microorganisms 10 (2022) 1–17, https://doi.org/10.3390/microorganisms10020351.
[60] M. Koch, K.W. Berendzen, K. Forchhammer, On the role and production of polyhydroxybutyrate (PHB) in the cyanobacterium Synechocystis sp. pcc 6803, Life 10 (2020), https://doi.org/10.3390/life10040047.
[61] M. Koch, J. Bruckmoser, J. Scholl, W. Hauf, B. Rieger, K. Forchhammer, Maximizing PHB content in Synechocystis sp. PCC 6803: a new metabolic engineering strategy based on the regulator PirC, Microb. Cell Fact. 19 (2020) 1–12, https://doi.org/10.1186/s12934-020-01491-1.
[62] S. Crognale, B. Tonanzi, F. Valentino, M. Majone, S. Rossetti, Microbiome dynamics and phaC synthase genes selected in a pilot plant producing polyhydroxyalkanoate from the organic fraction of urban waste, Sci. Total Environ. 689 (2019) 765–773.
[63] R. Pei, G. Vicente-Venegas, M.C.M. Van Loosdrecht, R. Kleerebezem, A. Werker, Visualization of polyhydroxyalkanoate accumulated in waste activated sludge, Water Res. 221 (2022), https://doi.org/10.1016/j.watres.2022.118795.